

COMPUTER CODE PREDICTION OF PICOSECOND VOLTAGE SWITCHING
AND TEM WAVE GENERATION IN AIR GAS AVALANCHE SWITCHES*

D. J. Mayhall and J. H. Yee
Lawrence Livermore National Laboratory
University of California
P. O. Box 808, L-156
Livermore, CA 94550

F. Villa
Stanford Linear Accelerator Center
P. O. Box 4349, Mail Bin 65
Stanford, CA 94305

Introduction

The realization of efficient, reliable picosecond closing switches will make possible high gradient (1-3 GeV) linacs with pulsed accelerating electrode structures. Recently a promising candidate for picosecond, high voltage switching, the gas avalanche switch, has been proposed.^{1,2} The medium in this switch is high pressure (10-800 atm) gas. An avalanche discharge is initiated between pulse-charged high voltage electrodes by multiphoton ionization from a picosecond order laser pulse. The laser-initiated electrons avalanche toward the anode, causing the applied voltage to collapse in picoseconds, long before the hot current channel formation of a conventional spark gap.

Several versions of the gas avalanche switch may be conceived. A parallel plate capacitor version consists of a high pressure gas confined between two parallel metal plates. An analysis of the formation or voltage delay and voltage collapse times for this geometry has been done by Villa and Cassell^{1,2} by numerical integration of a zero-dimensional (0D) electric circuit equation, which includes a resistively limited charge feed. This analysis predicts voltage collapse times of the order of several picoseconds for N₂ and air and 1 psec or less for Ar.

The Two-Dimensional Electromagnetic
Electron Fluid Avalanche Code

For confirmation of the encouraging results of the circuit code, we have written a two-dimensional (2D) code, which simultaneously and selfconsistently solves Maxwell's equations for transverse magnetic (TM) field modes in a gas between two parallel perfect conductors and a set of electron fluid conservation equations. A rectilinear perfect conductor may be placed between the plates.

For a free space dielectric between the plates, the relevant Maxwell's equations in the MKS system are

$$\frac{\partial E_x}{\partial t} = \frac{1}{\epsilon_0} \frac{\partial H_z}{\partial y} - \frac{nev_x}{\epsilon_0} \quad (1)$$

$$\frac{\partial E_y}{\partial t} = -\frac{1}{\epsilon_0} \frac{\partial H_z}{\partial x} - \frac{nev_y}{\epsilon_0} \quad (2)$$

$$\frac{\partial H_z}{\partial t} = -\frac{1}{\mu_0} \frac{\partial E_y}{\partial x} + \frac{1}{\mu_0} \frac{\partial E_x}{\partial y} \quad (3)$$

where E_x is the electric field in the x direction, E_y is the electric field in the y direction, H_z is the magnetic field in the z direction (the unmodeled direction perpendicular to x and y), ε₀ is the

permittivity, n is the electron density, e is -1.6 x 10⁻¹⁹ coul, v_x is the electron velocity in the x direction, v_y is the electron velocity in the y direction and μ₀ is the permeability.

The electron fluid equations for continuity, momentum, and energy conservation are

$$\frac{\partial n}{\partial t} = nv_i \quad (4)$$

$$\frac{\partial (nv_x)}{\partial t} = \frac{neE_x}{m} - nv_m v_x \quad (5)$$

$$\frac{\partial (nv_y)}{\partial t} = \frac{neE_y}{m} - nv_m v_y \quad (6)$$

$$\frac{\partial (nU)}{\partial t} = ne(E_x v_x + E_y v_y) - nv_u (U - U_0) - nv_i \epsilon_i \quad (7)$$

where v_i is the ionization collision frequency, m is the electron mass, v_m is electron-neutral molecule momentum transfer frequency, U is the average electron kinetic energy, v_u is electron-neutral energy transfer frequency, U₀ is the average neutral energy, and ε_i is the neutral ionization potential. The equations are specialized to air by taking U₀ = 0.025 eV and ε_i = 14 eV. It must be noted that convection, pressure gradients, heat flow, and magnetic forces are neglected. Electron losses due to atomic and molecular processes, such as attachment and recombination, are ignored. Electron generation from photoionization is also ignored.

The collision frequencies for air are those used previously in microwave breakdown calculations.³ These frequencies are assumed to scale linearly with neutral pressure. In addition electrode pulse charging is assumed to be instantaneous so that the very real experimental problem of premature breakdown due to effects, such as field emission, is ignored. The initial laser deposition of electrons is also assumed instantaneous. Thus the details of modeling the laser ionization are presently conveniently bypassed.

The space between the horizontal parallel plates is partitioned with a rectangular mesh. Solution points for the electromagnetic and fluid variables are sited to obtain a staggered grid, similar to those in explicit, 2D, finite difference, electromagnetic scattering codes. E_x is solved at even points along odd horizontal (xz) planes. The lowest of these planes coincides with the bottom metal plate; whereas, the uppermost plane coincides with the top capacitor plate. E_y is solved at odd points along even horizontal planes; whereas, H_z is solved at even points on the same planes. The four fluid variables are

*This work was performed under the auspices of the U.S. Department of Energy by the Lawrence Livermore National Laboratory under Contract W-7405-Eng-48.

Report Documentation Page

Form Approved
OMB No. 0704-0188

Public reporting burden for the collection of information is estimated to average 1 hour per response, including the time for reviewing instructions, searching existing data sources, gathering and maintaining the data needed, and completing and reviewing the collection of information. Send comments regarding this burden estimate or any other aspect of this collection of information, including suggestions for reducing this burden, to Washington Headquarters Services, Directorate for Information Operations and Reports, 1215 Jefferson Davis Highway, Suite 1204, Arlington VA 22202-4302. Respondents should be aware that notwithstanding any other provision of law, no person shall be subject to a penalty for failing to comply with a collection of information if it does not display a currently valid OMB control number.

1. REPORT DATE JUN 1989	2. REPORT TYPE N/A	3. DATES COVERED -	
4. TITLE AND SUBTITLE Computer Code Prediction Of Picosecond Voltage Switching And Tem Wave Generation In Air Gas Avalanche Switches		5a. CONTRACT NUMBER	
		5b. GRANT NUMBER	
		5c. PROGRAM ELEMENT NUMBER	
6. AUTHOR(S)		5d. PROJECT NUMBER	
		5e. TASK NUMBER	
		5f. WORK UNIT NUMBER	
7. PERFORMING ORGANIZATION NAME(S) AND ADDRESS(ES) Lawrence Livermore National Laboratory University of California P. O. Box 808, L-156 Livermore, CA 94550		8. PERFORMING ORGANIZATION REPORT NUMBER	
		10. SPONSOR/MONITOR'S ACRONYM(S)	
9. SPONSORING/MONITORING AGENCY NAME(S) AND ADDRESS(ES)		11. SPONSOR/MONITOR'S REPORT NUMBER(S)	
		12. DISTRIBUTION/AVAILABILITY STATEMENT Approved for public release, distribution unlimited	
13. SUPPLEMENTARY NOTES See also ADM002371. 2013 IEEE Pulsed Power Conference, Digest of Technical Papers 1976-2013, and Abstracts of the 2013 IEEE International Conference on Plasma Science. Held in San Francisco, CA on 16-21 June 2013. U.S. Government or Federal Purpose Rights License.			
14. ABSTRACT			
15. SUBJECT TERMS			
16. SECURITY CLASSIFICATION OF:			17. LIMITATION OF ABSTRACT SAR
a. REPORT unclassified	b. ABSTRACT unclassified	c. THIS PAGE unclassified	
			18. NUMBER OF PAGES 4
			19a. NAME OF RESPONSIBLE PERSON

solved at points where H_z is defined. The spatial derivatives in Maxwell's equations are replaced with central finite differences. Seven ordinary differential equations in time result for each grid cell of four grid points. The global set of equations for all the grid cells is solved by time integration with the block-iterative, stiff, implicit, variable step solver GEARBI.⁴

Modeling Parallel Plate Capacitor Switches

The 2D avalanche code was first applied to a parallel plate capacitor with a spacing or gap of 100μ and an extent in the x direction of 247.5μ . An initial electron number of 10^{10} ($n = 4 \times 10^{11} \text{ m}^{-3}$) was uniformly distributed for an assumed depth of 1 m in the z direction. A voltage of 266 kV was applied to the top plate by initialization of a spatially uniform E_y . Boundary conditions were applied at $x = 0$ and 247.5μ , which approximated the infinite extension of the parallel plate capacitor. An air pressure of 350 atm was specified, and the simulation was started.

The resulting plate voltage waveform is shown in Figure 1, labeled "2D Code." The voltage across the plates stays almost constant for about 3 psec, then decays exponentially. The voltage collapse time is about 2 psec. The result of a circuit code calculation by Cassell and Villa² is shown as the curve labeled "Circuit Code." For this calculation, the first Townsend coefficient α was set to 2/3 of its reported experimental value.

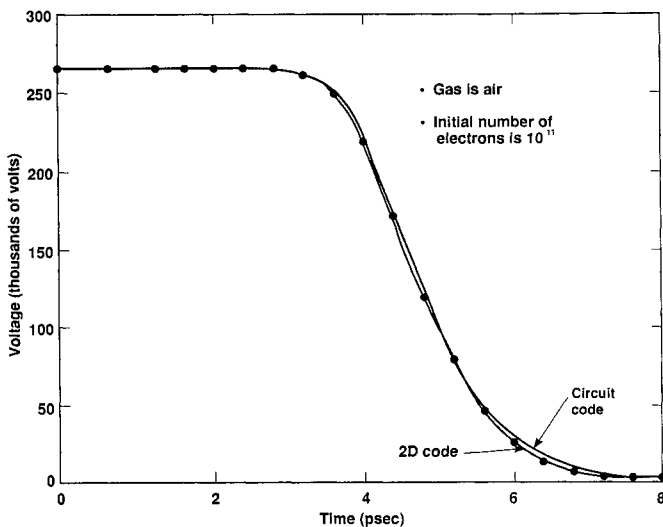


Figure 1. Comparison of voltage waveforms at 266 kV and 350 atm. Alpha is the first Townsend coefficient used in the circuit code calculations and is equal to 0.67 times the reported value.

This adjustment is supported by Figure 2, which shows the ratio of the pressure-normalized first Townsend coefficient α/p from the 2D Code to that from experimental data.⁵ The quantity p is the neutral gas pressure in Torr. The stored electric field energy is also shown as a percentage of the initial electrostatic field energy. Over most of the decay of the electric field energy, α from the 2D code is about 0.6-0.7 of the experimental value.

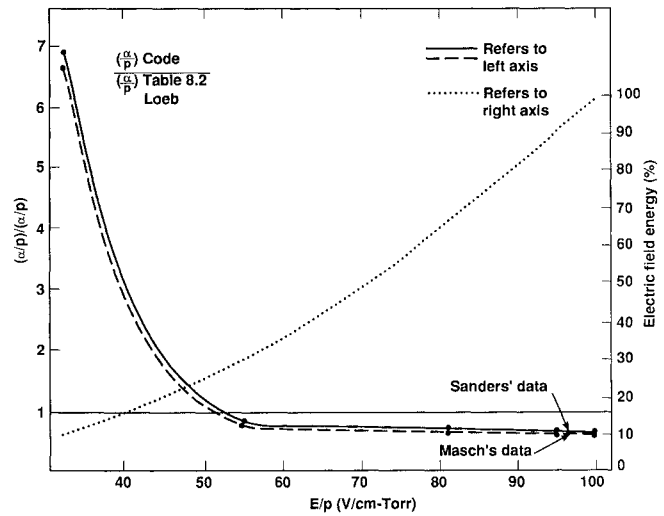


Figure 2. Ratio of $\frac{\alpha}{p}$ for the code to measured $\frac{\alpha}{p}$.

Figure 3 shows the average electron velocity from the 2D code versus E/p for the range 0.1 - 16.5 V/(cm-Torr). The electron drift velocity measured by Bradbury and Nielsen⁶ is also shown. The agreement of the two curves is excellent.

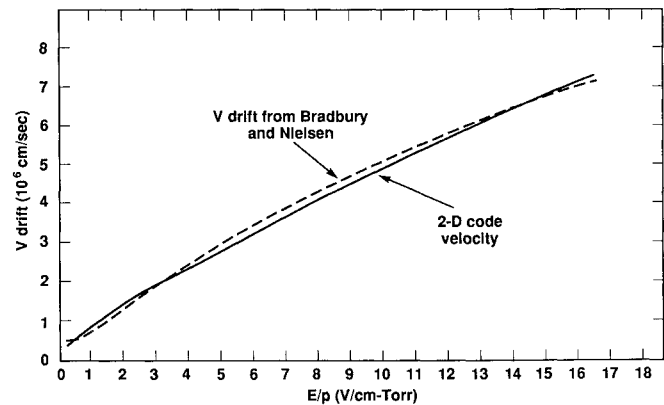


Figure 3. Comparison of electron drift velocities.

Figure 4 shows the change of the capacitor voltage waveform with pressure at constant initial voltage and electron number. The initial E/p is shown with each pressure. As the air pressure increases and the initial E/p consequently decreases, both the delay time and the voltage collapse time increase.

Further calculations show picosecond scale delay and collapse times on the same 100μ plane gap at lower and, hence more experimentally appealing, charging voltages. At 10^{10} initial electrons/m of plate depth, 80 kV, and 27.2 atm, the voltage delay time is 2.2 psec; the decay time is 1.8 psec. At the same electron number, 62 kV, and 17.0 atm, the delay time is 2.3 psec; the decay time is 1.7 psec. At 43 kV and 10.2 atm, the delay time is 2.8 psec, and the decay time is 2.1 psec. These conditions of voltage and pressure are relevant because, in recent preliminary experimental work with N_2 , a pulse-charged 102μ curved to knife edge gap has withheld these voltages for 6 nsec with an irregular ac pulse.

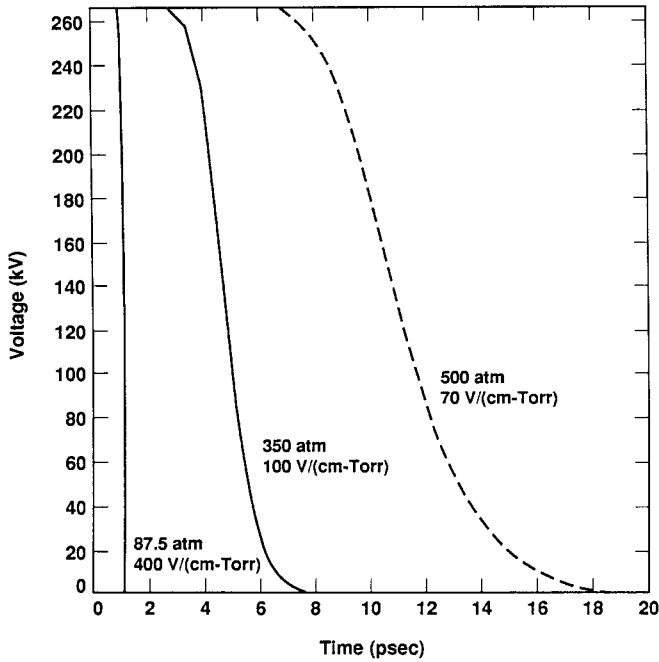


Figure 4. Voltage waveforms versus air pressure.

Modeling TEM Wave Generating Accelerator Switches

A more sophisticated gas avalanche switch, suitable for a pulsed power linac, can be made by placing a properly dimensioned center electrode between the parallel plates and charging it to a suitable high voltage. A simple model of such a linac switch is shown in Figure 5. The parallel plates are initially grounded; the air between them is at 700 atm. The gap between the center electrode and the bottom plate is uniformly filled with 1.7×10^{13} electrons for an assumed depth of 1 m into the figure. For a center electrode voltage of 3.889 MV, this configuration produces electromagnetic waves, which are predominantly

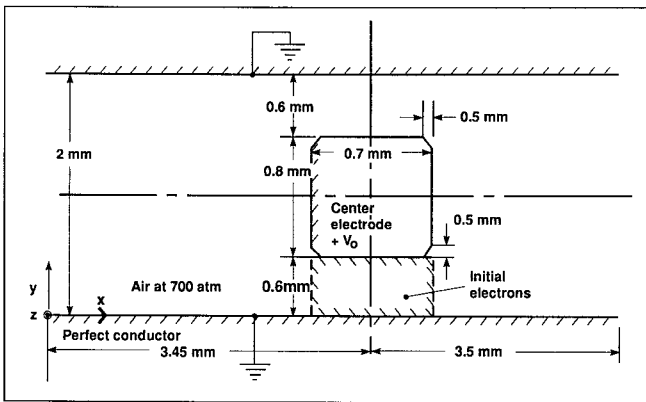


Figure 5. The accelerator switch model.

TEM modes and propagate outward from the center electrode to the left and right boundaries.

The initial electric field components E_x and E_y are obtained from the finite element, electrostatic code STAT2D and used as initial conditions for the electron avalanche code. After the simulation starts, the voltage between the center electrode and the lower plate collapses within 1 psec. Avalanche-generated E_y waves at 10 psec are shown in Figure 6. The wave

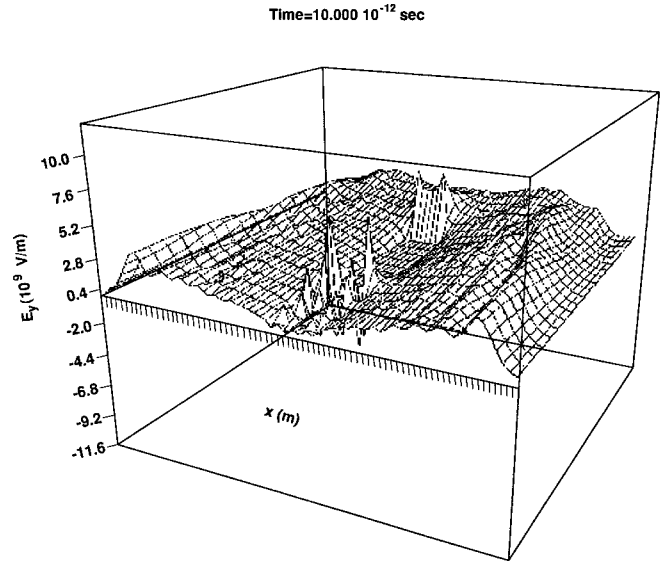


Figure 6. E_y at 10 psec.

crests in the near E_y -x plane, which corresponds to the lower parallel plate, will hit the x boundaries at about 12 psec. The wave crests in the far E_y -x plane, which corresponds to the top plate, lag behind those in the near E_y -x plane. The bipolar spikes below the center electrode are from H_z noise introduced from inaccuracies in the extrapolated STAT2D electric fields at the center electrode surface. In addition to the strong E_y waves, weak E_x waves propagate from the center electrode.

The voltage waveform of the top plate with respect to the lower plate at the right boundary is shown as the solid curve in Figure 7, where the rise time is less than 2 psec. The first peak is from the crest at the lower plate; the second peak is from the lagging crest at the top plate. The voltage full width at half

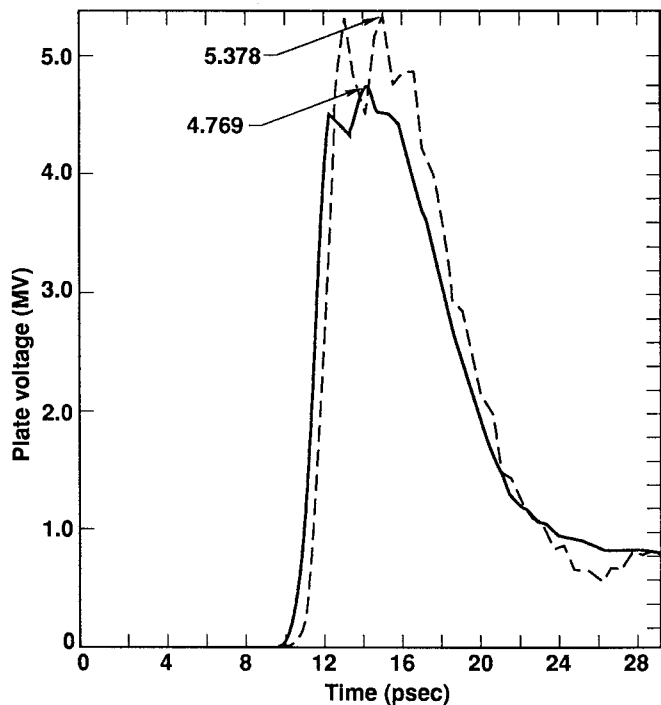


Figure 7. Plate voltage waveform at the right boundary.

maximum (fwhm) is about 8 psec. The peak voltage of 4.769 MV is a 22.6 % enhancement of the initial center electrode voltage. This enhancement is most likely due to the transmission properties of the transmission line transitions at the sides of the center electrode, where two short, separated narrow lines join a wider line. At 29.5 psec, 422 J or 71.4 % of the initial electrostatic energy has been transported across the boundaries.

When 1.2×10^{12} initial electrons are evenly concentrated into a 50 μ wide column centered under the center electrode, a peak right boundary voltage of 5.378 MV and the dashed waveform in Figure 7 result. This is a 38.3 % voltage enhancement. In this case 490 J or 82.9 % of the initial energy has been transported out of the computational space by 29.5 psec.

Further simulations predict that, without convection or photoionization, the center electrode to lower plate space must be completely bridged by initial electrons for maximal voltage pulse generation and energy transport. If 1.7×10^{13} initial electrons are concentrated uniformly in the two thirds of that space closest to the center electrode, then the peak pulse voltage is 3.15 MV, and the energy transport is 20 %. If the same initial electrons are concentrated uniformly in the one third of that space closest to the center electrode, then the peak pulse voltage is 2.11 MV and the energy transport is 9.4 %.

The previously mentioned experimental work has shown encouraging voltage holdoff in N_2 at 80 kV and 27.2 atm. These conditions represent an initial plane gap E/p of 379 V/(cm-Torr). At 300 kV and 27.2 atm, the initial nominal center electrode E/p on the accelerator switch in Figure 5 is 386 V/(cm-Torr) with a 600 μ gap. A simulation at these conditions, where there is greater expectation for sufficient voltage holdoff time, produces a boundary voltage pulse of 2.5 psec risetime and about 9 psec fwhm. The peak pulse voltage is 301 kV and the energy transport is 55.4 % at 36.5 psec.

Conclusions

The parallel plate, 2D electron fluid avalanche code predicts voltage collapse times of 1-10 psec for air pressures of 80-500 atm. The collapse times agree well with OD circuit code results. The electron drift velocity from the 2D code agrees well with experimental results for $0.1 \leq E/p \leq 16$ V/(cm-Torr). The α/p from the 2D code is in good agreement with experimental results for $46 \leq E/p \leq 100$ V/(cm-Torr). Simulations at lower voltages and pressures, for which there are some promising preliminary experimental results for voltage holdoff at the same nominal electrode gap, also give picosecond scale (1.7-2.1) voltage collapse times.

A linac switch structure with a parallel plate spacing of 2 mm, a pressure of 700 atm air, an initial nominal center electrode E/p of 200 V/(cm-Torr) and a charging voltage of 3.889 MV produces voltage collapse in less than 1 psec and TEM wave generation. Transmitted voltage pulse risetimes of 2 psec, voltage pulse enhancements of 23-38 %, and energy transports of 71-83 % of the initial electric field energy are predicted. Lower voltages (300 kV) and pressures (27 atm) on this very same switch structure give similar results.

References

- [1] F. Villa, "High Gradient Linac Prototype: A Modest Proposal," SLAC-PUB-3875, January 1986.
- [2] R. E. Cassell and F. Villa, "High Speed Switching In Gases," SLAC-PUB-4858, February 1989; Proc. 4th Workshop: Pulse Power Techniques for Future Accelerators, Erice, Trapani, Italy, March 4-9, 1988; to be published by Plenum Press.
- [3] D. J. Mayhall, J. H. Yee, R. A. Alvarez, and D. P. Byrne, Laser Interaction and Related Plasma Phenomena, G. Miley and H. Hora, eds., New York: Plenum Press, 1988, pp. 121-137.
- [4] A. C. Hindmarsh, "Preliminary Documentation of GEARBI: Solution of ODE Systems with Block-Iterative Treatment of the Jacobian," UCID-30149, Lawrence Livermore National Laboratory, Livermore, CA, 1976.
- [5] L. B. Loeb, Basic Processes of Gaseous Electronics, Berkeley and Los Angeles: University of California Press, 1960, p. 676.
- [6] Previous book, p. 231.